Metrol. Meas. Syst., Vol. 26 (2019) No. 3, pp. 531–540
DOI: 10.24425/mms.2019.129577

METROLOGY AND MEASUREMENT SYSTEMS
Index 330930, ISSN 0860-8229
www.metrology.pg.gda.pl

DEVELOPMENT OF A TECHNIQUE FOR INDUCTIVE MEASUREMENT OF LASER-INDUCED MAGNETIZATION DYNAMICS IN THIN FILMS

Tomáš Ilit'[1)], Pavol Valko[1)], Milan Držík[2)], Marianna Ušáková[1)], Martin Šoka[1)], Marian Marton[1)], Miroslav Behúl[1)], Marian Vojs[1)]

1) *Slovak University of Technology, Faculty of Electrical Engineering and Information Technology, Ilkovičova 3, 81219 Bratislava, Slovakia* (✉ *i.tomas007@gmail.com*, +421 2 602 91 111, *pavol.valko@stuba.sk*, *marianna_usakova@stuba.sk*, *martin.soka@stuba.sk*, *marian.marton@stuba.sk*, *miroslav.behul@stuba.sk*, *marian.vojs@stuba.sk*)
2) *International Laser Centre, Ilkovičova 3, 841 04 Bratislava, Slovakia* (*Drzik@ilc.sk*)

Abstract

We present the development of a technique for studying laser-induced magnetization dynamics, based on inductive measurement. The technique could provide a simple tool for studying laser-induced demagnetization in thin films and associated processes, such as Gilbert damping and magnetization precession. It was successfully tested using a nanosecond laser and NiZn ferrite samples and – after further development – it is expected to be useful for observation of ultra-fast demagnetization. The combination of optical excitation and inductive measurement enables to study laser-induced magnetization dynamics in both thin and several micrometre thick films and might be the key to a new principle of ultrafast broadband UV–IR pulse detection.

Keywords: laser-induced demagnetization, pulsed inductive microwave magnetometry, ultrafast demagnetization detection.

1. Introduction

Since the discovery of ultrafast magnetization processes under femtosecond laser excitation [1], various magnetic materials in forms of thin films, nanoparticles, and micro and nanostructures were studied with regard to fast laser-induced magnetization dynamics [2–5]. Ultrafast magnetization dynamics is important for future magnetic storage devices and applications in spintronics, therefore a lot of research effort is being put into this field. Numerous techniques, such as *time-resolved magneto-optic Kerr effect* (TR-MOKE) [6], *time-resolved x-ray magnetic circular dichroism* (TR-XMCD) [7], or *pulsed inductive microwave magnetometry* (PIMM) [8] were developed to study ultrafast magnetization dynamics in thin films. These techniques provide femtosecond time resolution and spatial resolution up to tens of nanometres (TR-XMCD).

In general, they can be divided into techniques based on optical and electrical measurements, although a combination of both exists. A combination of a current-induced field pulse and optical

measurement is used in time-resolved scanning Kerr microscopy [9]. However, there was no measurement technique reported to use ultrafast laser excitation in combination with electrical, namely inductive, measurement.

One of the reasons might be a limited time resolution of inductive measurements, in comparison with optical measurement techniques. Time resolution of PIMM technique, as well as of any direct inductive measurement, is limited by electronics to approx. 5 ps, considering a 100 GHz oscilloscope [10]. Such a time resolution is sufficient for studying Gilbert damping in thin films or laser induced magnetization precession and is useful for studying magnetization dynamics of microscale and nanoscale objects [11], regardless of surface texture and reflectivity that are limiting optical techniques.

Using a femtosecond laser and a variable time delay between trigger and signal pulse, such as in MOKE measurements [12], it might be possible to increase time resolution and enable to observe ultrafast magnetization dynamics using this method.

In this work we present initial experimental results and discuss both limitations and potential of a measurement technique combining laser excitation and inductive pick-up.

2. Measurement setup

2.1. Experimental setup

The setup consisted of a CryLas laser with a pulse width FWHM < 1.3 ns and pulse energy values of 4 μJ/5.5 μJ for 532/1064 nm wavelengths, respectively, two 20 dB PAM102 amplifiers rated up to 2 GHz, a silicon PIN diode detector Thorlabs Det 10A and a LeCroy WaveMaster 808Zi oscilloscope with a sampling rate of 40 GS/s. Optical components and samples were mounted on an optical table. The setup is shown in Fig. 1.

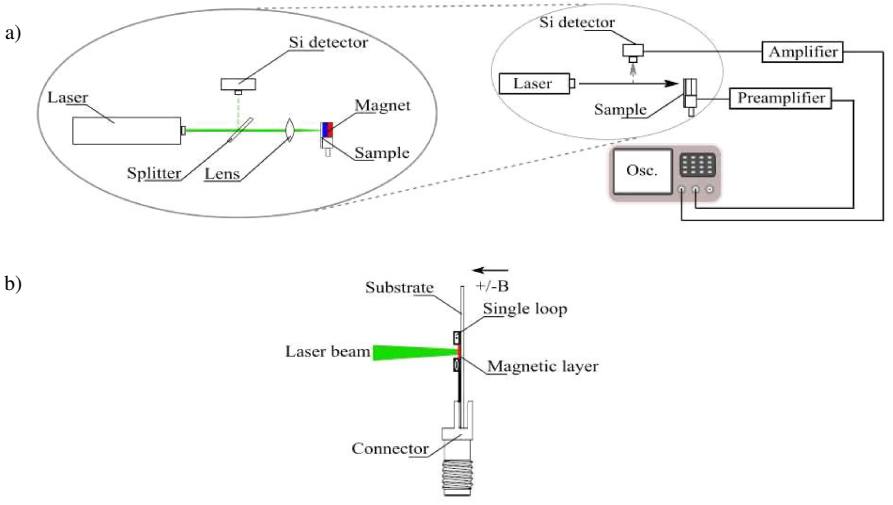

Fig. 1. A block scheme of the experimental setup (a) and a close-up of the sample under external magnetic field perpendicular to the sample plane (b).

The signal from the semiconductor diode detector was used as the trigger signal. Most of the measurements were carried out with green 532 nm wavelength, due to better visibility of the

Metrol. Meas. Syst., Vol. 26 (2019), No. 3, pp. 531–540
DOI: 10.24425/mms.2019.129577

laser spot and thus ease of manipulation. There was no significant difference observed between demagnetizing effects of both the wavelengths. A collimating lens was used in most of the experiments in order to concentrate the laser power and decrease the beam spot size down to approximately 0.3 mm, resulting in average fluence of 17.8 mJ/cm^2 per pulse for the sample. The pulse frequency of the laser was adjustable in a range of 1 Hz–20 kHz. A neodymium permanent magnet was used as the source of a stable external magnetic field, providing nearly uniform field of approximately 0.2 T in the sample. Signal averaging was used in addition to 40 dB amplification, in order to improve signal to noise ratio, resulting in practical detection limits below 20 μV at 1 GHz.

2.2. Samples

The samples used to test the measurement setup were based on $Ni_{0.33}Zn_{0.67}Fe_2O_4$ in the form of powder with 40 and 200 μm grain sizes, and 160 nm thick film, $Ni_{0.3}Zn_{0.7}Fe_2O_4$ in the form of 1 μm thick film and $(Fe_1Ni_3)_{81}Nb_7B_{12}$ in the form of amorphous, Cu-ion doped 25 μm thick foil.

An SEM picture of the deposited 160 nm thick Nickel–Zinc ferrite layer is shown in Fig. 2, together with the dependence of susceptibility on temperature, which was measured for both ferrite materials using the TGA method.

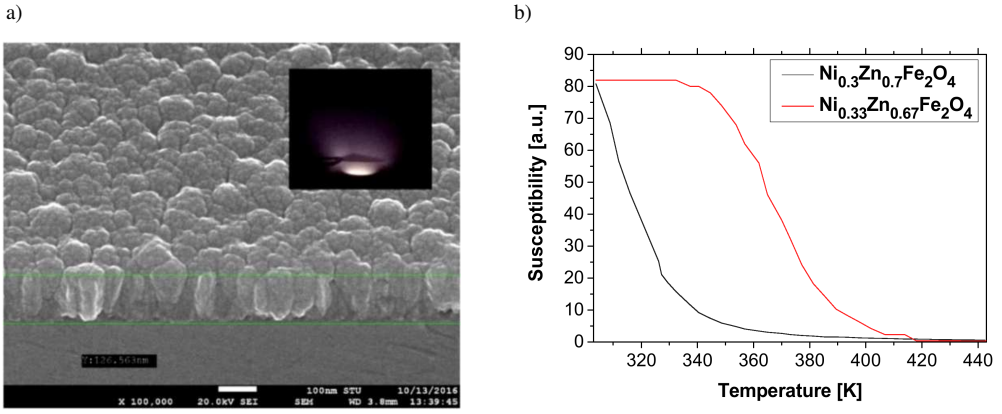

Fig. 2. An SEM image of the 160 nm thick $Ni_{0.33}Zn_{06.7}Fe_2O_4$ taken from approx. 45° angle together with the footage from the sputtering process (a) and susceptibility vs. temperature for $Ni_{0.3}Zn_{0.7}Fe_2O_4$ and $Ni_{0.33}Zn_{0.67}Fe_2O_4$ (b).

As it can be seen from the characteristics, Curie temperatures of $Ni_{0.3}Zn_{0.7}Fe_2O_4$ and $Ni_{0.33}Zn_{0.67}Fe_2O_4$ are around 313 K and 363 K, or 40°C and 90°C, respectively. The Curie temperature of the amorphous $(Fe_1Ni_3)_{81}Nb_7B_{12}$ was also around 90°C.

The sample materials were deposited on single loop inductors prepared on an FR4 substrate using photolithography. The 160 nm thick $Ni_{0.33}Zn_{0.67}Fe_2O_4$ layer was prepared on a silicon substrate and annealed at 600°C for 8 hours, in order to retain magnetic properties of the sputtering target. The single loop diameter varied from 0.6 to 2 mm and bare loop antennas had minimal return loss around 4 and 3 GHz, respectively. The 160 nm and 1 μm thick layers were deposited using magnetron sputtering in a vacuum installation of UVNIPA-1-001 type, described in [13], while all other sample materials were bonded to the substrate using a silicon-based bonding agent.

2.3. Working principle

To describe ultrafast magnetization phenomena, three temperature models were used. However, due to a relatively long pulse duration of the tested laser, in the order of ns, in comparison with the electron-phonon coupling constant in the order of 1–10 picoseconds, the change of magnetization is governed mostly by heat diffusion. Solving the Fourier-heat equation:

$$\frac{\mathrm{d}\mathbf{u}}{\mathrm{d}t} - \alpha\Delta\mathbf{u} = 0, \tag{1}$$

where Δ is Laplace operator; α is thermal diffusivity and $u(x, y, z, t)$ temperature function, the temperature profile and its time evolution can be calculated. A change in temperature causes a change in magnetic susceptibility, which is described by the Curie-Weiss law in the paramagnetic region and can be described by means of the mean-field theory in the ferromagnetic region. A change in susceptibility of the heated region causes a time variation of the magnetic flux passing through the pick-up loop and thus – according to the 3rd Maxwell equation – a voltage induced in the inductor. The upper limit of the demagnetized volume by a single pulse for film thickness much higher than the incident light wavelength, can be expressed as:

$$V_{\max} = \frac{(1-R)E}{c\rho(T_c - T_s)}, \tag{2}$$

where R is reflectance of the surface; E is energy per pulse; c specific heat; ρ density; T_c Curie temperature and T_s sample temperature. For more precise calculation, or for a series of pulses, heat propagation has to be accounted for and the problem has to be solved numerically.

After the prompt laser pulse, heat transport, magnetization precession and other transient processes become the driving factors of the magnetization change.

3. Initial measurements

To prove the thermomagnetic origin of the laser-induced demagnetization signal measured by the measurement loop, measurements with magnetic field, without magnetic field and with magnetic field direction reversed were performed. The measured signal was reversed for reversed field direction as expected and no signal was measured in the experiment without external magnetic field, as the NiZn ferrites are magnetically soft.

Characteristics measured for $Ni_{0.33}Zn_{0.67}Fe_2O_4$ are shown in Fig. 3.

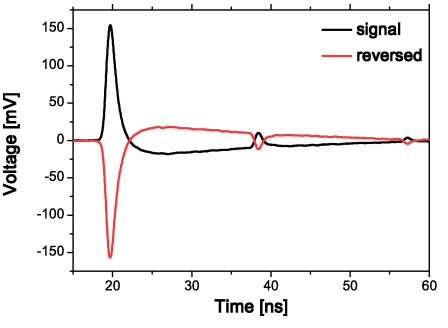

Fig. 3. An induced voltage signal measured during laser-induced demagnetization of $Ni_{0.33}Zn_{0.67}Fe_2O_4$ powder sample with 40 μm grain size deposited on 0.6 mm diameter loop inductor under external field perpendicular to the sample plane (signal) and with the field direction reversed (reversed).

Metrol. Meas. Syst., Vol. 26 (2019), No. 3, pp. 531–540
DOI: 10.24425/mms.2019.129577

The delay between the trigger pulse delivered by the triggering detector and the signal is produced by the amplifiers, which require several nanoseconds to amplify the signal. We suspect also that the small peaks of repetitive pulses visible in the measured characteristic can be caused by the amplifier electronics. The prompt peak was however confirmed to be proportional to the measured signal amplitude using a comparative measurement with a different amplifier – a 40 dB Minicircuits ZKL-1R5+. Nevertheless, optimization of the amplification is needed to better reproduce the demagnetization-induced voltage pulse shape.

The thermomagnetic signal amplitude is dependent on the sample temperature. When the sample temperature is close to its Curie temperature, the volume of the region demagnetized by a single pulse is increased, as well as the magnitude of field change. The measured signal decreases again when the sample is heated above its Curie temperature, defined as the maximum slope of the temperature dependence of susceptibility. By varying frequency of the laser pulses, we varied the amount of heating power delivered to the sample and thus the sample temperature. As it can be seen in Fig. 4, the measurements confirmed increasing the signal with increasing the pulse frequency up to a threshold, associated with Curie temperature of the sample, and decreasing the signal after further increasing the pulse frequency.

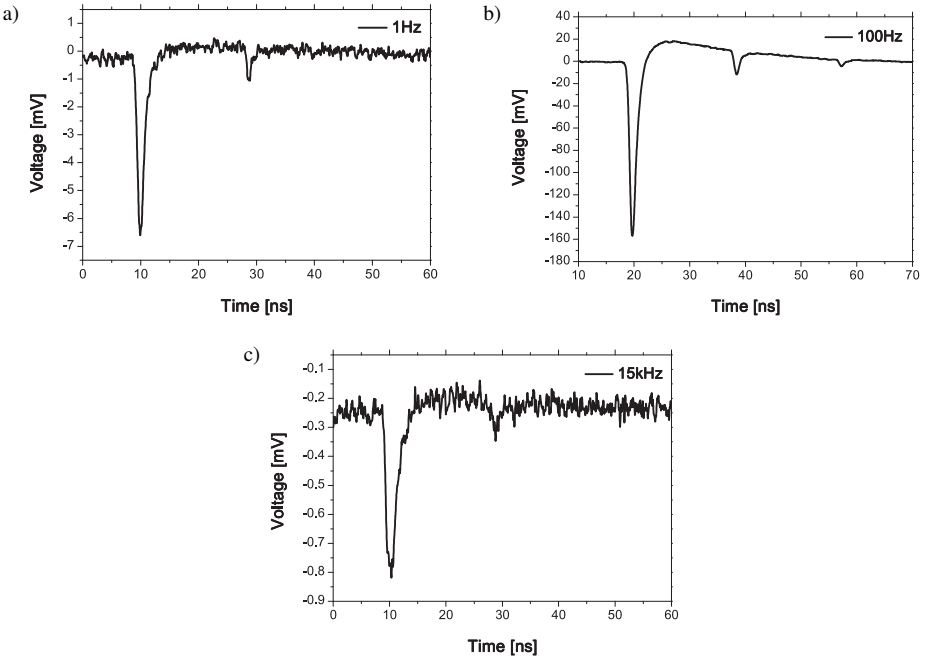

Fig. 4. Fig. 4. An induced voltage signal measured during laser-induced demagnetization of $Ni_{0.33}Zn_{0.67}Fe_2O_4$ powder sample with 40 μm grain size deposited on 0.6 mm diameter loop inductor under external field perpendicular to the sample plane under pulse frequency of 1 Hz (a), 100 Hz (b), and 15 kHz (c).

The temperature measurement in the laser spot would be difficult due to the system not being in thermal equilibrium, therefore a test using a thermocouple heater was performed to confirm the signal decrease after heating the sample above its Curie temperature. When the sample temperature in the place of laser spot decreased below the Curie temperature, the change in susceptibility resulted in retaining the magnetization to the same level as before the laser pulse. This was observed in all experiments for all the used soft-magnetic materials.

Using (2) and considering the whole pulse energy being absorbed in a specified volume ($R = 0$), we can calculate the upper limit of the demagnetized volume of a ferromagnetic sample.

Assuming the 1 Hz pulse repetition rate a close approximation of a single pulse, the 200 μm thick $Ni_{0.33}Zn_{0.67}Fe_2O_4$ powder composite layer with 40 μm grain size, temperature of 20°C (NTP), specific heat of 750 $Jkg^{-1}K^{-1}$, density of 1300 kg/m^3 and Curie temperature of 90°C, shown in Fig. 6a would reach Curie temperature in a volume smaller than 5.86×10^{-5} mm^3. This is just a small fraction of the 6.2×10^{-1} mm^3 layer volume inside the measurement loop, proving observability of even partial demagnetization of the sample.

We further tested a thin film $Ni_{0.33}Zn_{0.67}Fe_2O_4$ sample, prepared by sputtering. The thin film was deposited on a Si substrate and the measured characteristic was compared with the thermomagnetic signal from 200 μm thick NiZn powder-silicon composite layer, obtained at the same conditions as shown in Fig. 5a.

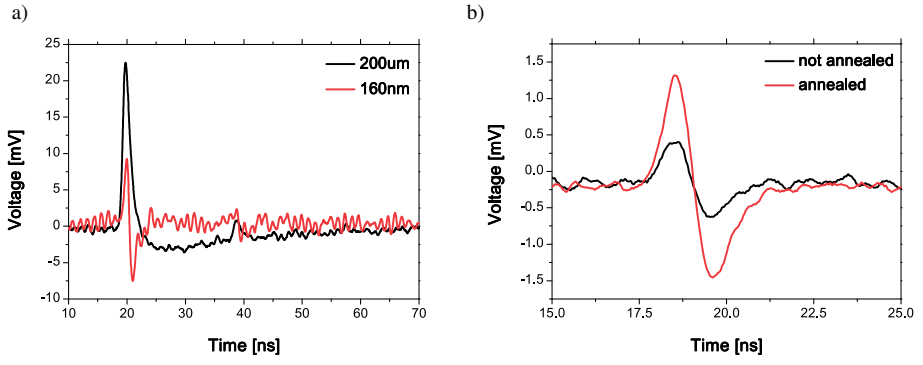

Fig. 5. A signal from a 160 nm $Ni_{0.33}Zn_{0.67}Fe_2O_4$ layer compared with a signal from a 200 μm layer of the same chemical composition, both measured with 2 mm diameter inductor (a) and a voltage signal measured with 1 μm thick $Ni_{0.3}Zn_{0.7}Fe_2O_4$ layer before (not annealed) and after annealing, deposited also on an inductor with 2 mm diameter (b).

The difference in the demagnetization peak shape of the 160 nm and 200 μm NiZn layers could be explained by damped precession, observed for thin films of certain compounds in ultrafast demagnetization experiments with a femtosecond laser [12] and the difference in magnitude might be due to different reflectivity of the samples as thickness of the thin film is smaller than the incident wavelength. Nevertheless, the measurement confirmed demagnetization of the thin film to be detectable and the demagnetization peak shape similar to that of the 160 nm layer was observed also for 1 μm layer of the $Ni_{0.3}Zn_{0.7}Fe_2O_4$ deposited by magnetron sputtering, as shown in Fig. 5b, where the as-deposited and annealed layers of the tested ferrite are compared.

Further experiments were focused on proving detection of magnetic anisotropy, which was present in a thin $(Fe_1Ni_3)_{81}Nb_7B_{12}$ Cu-ion doped foil, but not in the NiZn powder composite sample with 40 μm grain size, as shown in Fig. 6.

Different amplitudes of the demagnetization induced pulses measured for the NiZn ferrite powder sample, shown in the Fig. 6, were later found to have been caused by a smaller external field value in the measurement with field parallel to the sample plane.

In Fig. 7, the magnetization precession of Cu-ion doped $(Fe_1Ni_3)_{81}Nb_7B_{12}$ is shown. The precession lasted up to several tens of nanoseconds after the prompt pulse. The precession was observed for external magnetic field values near and under the saturation of magnetization of $(Fe_1Ni_3)_{81}Nb_7B_{12}$ alloy.

Metrol. Meas. Syst., Vol. 26 (2019), No. 3, pp. 531–540
DOI: 10.24425/mms.2019.129577

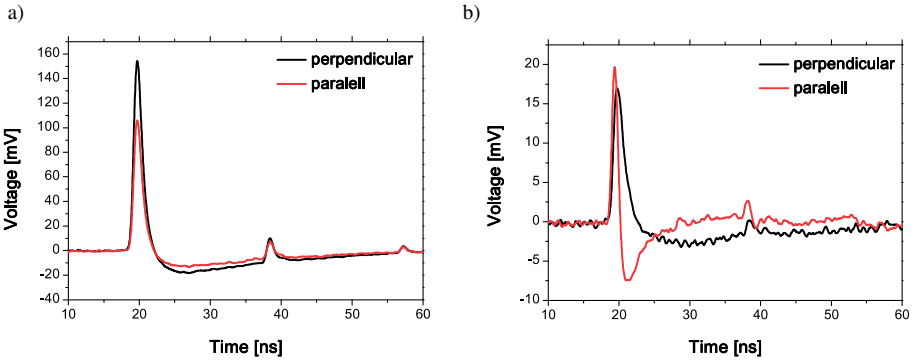

Fig. 6. Comparison of the and $Ni_{0.33}Zn_{0.67}Fe_2O_4$ ferrite with 40 μm grain size (a) and $(Fe_1Ni_3)_{81}Nb_7B_{12}$ Cu-ion doped alloy (b) characteristics under perpendicular and parallel external field orientation, all measured with a 2 mm diameter loop inductor.

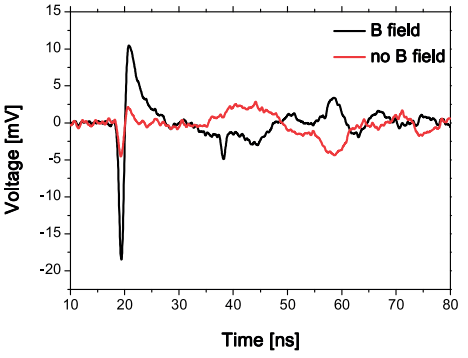

Fig. 7. A signal from $(Fe_1Ni_3)_{81}Nb_7B_{12}$ Cu-ion doped alloy on 2 mm diameter loop, with the external magnetic field parallel to the sample plane (B field) and shortly after removal of the external magnetic field (no B field).

All the characteristics are presented as measured, without further processing despite signal averaging during the measurement.

By comparing signals measured for the same magnetic material, using different inductors, it was found that the smaller the inductor diameter, the higher the measured voltage, suggesting that optimization of the inductor might provide further improvement in signal strength.

4. Discussion

4.1. Inductive vs. optical measurement

Magneto-optical Kerr effect (MOKE) is nowadays the most widely used method for observation of ultrafast magnetization. Although the method was developed to achieve high detection limits and doubts about its accuracy were resolved [14], compared to inductive measurement, it provides just indirect observation. On the other hand, inductive measurement is likely to have influence on the observed effect, therefore a simulation is needed to separate this influence.

For thick layers, optical measurement gives information mainly about surface magnetism, while inductive measurement provides information about the total magnetization change in the observed volume of the layer and is therefore useful for studying magnetization dynamics in both thin films and relatively thick ferromagnetic foils, such as the used 25 μm thick $(Fe_1Ni_3)_{81}Nb_7B_{12}$ Cu-ion doped foil. Such thick samples are routinely studied by PIMM technique [15], however using a fast magnetic field change instead of a laser pulse, to study magnetization dynamics. Although using a laser pulse to initiate a magnetization change induces a thermal gradient in the sample during measurement, it enables faster switching than PIMM or any other technique using alternating external magnetic field. A direct comparison of experimental results obtained using PIMM or MOKE and the described inductive technique is yet to be done, due to different excitation pulse lengths and materials used in the literature. The presented measurements carried out using a nanosecond laser are the first step towards inductive measurement of magnetization dynamics using femtosecond laser excitation, which might require further development of a suitable antenna and an increase of signal-to-noise ratio, to avoid high-frequency broadband amplification issues. Nevertheless, using a femtosecond laser and time resolution of the inductive measurement technique improved by an adjustable delay, it might be possible to inductively measure ultrafast magnetization processes. The inductive method provides a means to observe magnetization dynamics in samples regardless of surface roughness and reflectivity.

4.2. Limitations of inductive technique

In addition to the mentioned time resolution limitation of inductive measurement, due to the used electronics, impedance matching was found crucial for increasing detection limits [16]. This, together with amplifier electronics and antenna characteristics, limits the frequency range observable without distortion.

Amplification of a high-frequency broadband signal is a challenging task even with application of the state-of-the-art electronics. However, with precise triggering, time resolution can be increased using sampling methods similar to those used in MOKE measurements, namely a variable trigger delay. For optimized measurements with a high energy per centimetre squared per pulse and sample temperature close to the Curie temperature, amplification might not be needed.

However, a simulation or calibration might be required to directly relate the measured voltage to the absolute magnetization change.

4.3. Other potential applications

Due to the thermal nature of the effect and inductive pick-up, the magnetization dynamics is expected to be observable for a broad range of wavelengths, with magnitude varying as a function of surface reflectance of the magnetic layer. The initial tests confirmed partial demagnetization of the magnetic layer detectable as well as detection using nano-layers achievable. If confirmed to be sensitive to ultrafast demagnetization, the samples could be used as ultrafast broadband triggering detectors after improvement in signal to noise ratio.

Using ultrafast demagnetization, rise times in the order of picoseconds could be achievable with a well engineered magnetic antenna. Such a detector would find use in laser testing or as part of pump-probe experimental setups with a wavelength range from UV to IR. Therefore, its use as a detector is protected by a pending patent application.

Metrol. Meas. Syst., Vol. 26 (2019), No. 3, pp. 531–540
DOI: 10.24425/mms.2019.129577

5. Conclusions

The presented technique was successfully used to observe magnetization dynamics in both thin films and several micrometre thick foil samples at nanosecond time scale. It has the potential to provide a simple solution for observation of laser-induced magnetization dynamics and related processes. If confirmed to work using femtosecond laser irradiation, it might lead to development of ultrafast broadband triggering detectors and – using a femtosecond laser and a variable time delay of the trigger pulse – it might provide yet another means of studying ultrafast magnetization processes.

Acknowledgements

This work was supported by ESA PECS contract n. 4000116936/16/NL/NDe, by Slovak Research and Development Agency under the Project APVV-0088-12 and by the STU FEI grant scheme for young researchers.

References

[1] Beaurepaire, E., Merle, J.C., Daunois, A., Bigot, J.Y. (1996). Ultrafast spin dynamics in ferromagnetic nickel. *Phys. Rev. Lett.*, 76(22), 4215–4253.

[2] Ikemiya, K., Konishi, K., Fujii, E., Kogure, T., Kuwata-Gonokami, M., Hasegawa, T. (2014). Self-assembly and plasmon-enhanced ultrafast magnetization of Ag–Co hybrid nanoparticles. *Opt. Mater. Express.*, 4, 1564–1573.

[3] Mathias, S., La-O-Vorakiat, C., Shaw, J.M., Turgut, E., Grychtol, P., Adam, R., Rudolf, D., Nembach, H.T., Silva, T.J., Aeschlimann, M., Schneider, C.M., Kapteyn, H.C., Murnane, M.M. (2013). Ultrafast element-specific magnetization dynamics of complex magnetic materials on a table-top. *J. Electron Spectros. Relat. Phenomena*, 189, 164–170.

[4] Vodungbo, B., Gautier, J., Lambert, G., Sardinha, A.B., Lozano, M., Sebban, S., Ducousso, M., Boutu, W., Li, K., Tudu, B., Tortarolo, M., Hawaldar, R., Delaunay, R., Lopez-Flores, V., Arabski, J., Boeglin, C., Merdji, H., Zeitoun, P., Luning, J. (2012). Laser-induced ultrafast demagnetization in the presence of a nanoscale magnetic domain network. *Nat. Commun.*, 3, 1–6.

[5] Von Korff Schmising, C., Giovannella, M., Weder, D., Schaffert, S., Webb, J.L., Eisebitt, S. (2015). Nonlocal ultrafast demagnetization dynamics of Co/Pt multilayers by optical field enhancement. *New J. Phys.*, 17(3), 33047.

[6] Kirilyuk, A., Kimel, A.V., Rasing, T. (2010). Ultrafast optical manipulation of magnetic order. *Rev. Mod. Phys.*, 82(3), 2731–2784.

[7] Bonfim, M., Ghiringhelli, G., Montaigne, F., Pizzini, S., Brookes, N.B., Petroff, F., Vogel, J., Camarero, J., Fontaine, A. (2001). Element-selective nanosecond magnetization dynamics in magnetic heterostructures. *Phys. Rev. Lett.*, 86(16), 3646–3649.

[8] Gerrits, T., Schneider, M.L., Kos, A.B., Silva, T.J. (2006). Large-angle magnetization dynamics measured by time-resolved ferromagnetic resonance. *Phys. Rev. B – Condens. Matter Mater. Phys.*, 73(9), 094454.

[9] Hiebert, W.K., Stankiewicz, A., Freeman, M.R. (1997). Direct observation of magnetic relaxation in a small permalloy disk by time-resolved scanning kerr microscopy. *Phys. Rev. Lett.*, 79(6), 1134–1137.

[10] Chen, X., Chandrasekhar, S., Randel, S., Raybon, G., Adamiecki, A., Pupalaikis, P., Winzer, P.J. (2017). All-Electronic 100-GHz Bandwidth Digital-to-Analog Converter Generating PAM Signals up to 190 GBaud. *J. Light. Technol.*, 35(3), 411–417.

[11] Keatley, P.S., Kruglyak, V.V., Gangmei, P., Hicken, R.J. (2011). Ultrafast magnetization dynamics of spintronic nanostructures. *Philos. Trans. R. Soc. A Math. Phys. Eng. Sci.*, 369(1948), 3115–3135.

[12] Ganguly, A., Azzawi, S., Saha, S., King, J.A., Rowan-Robinson, R.M., Hindmarch, A.T., Sinha, J., Atkinson, D., Barman, A. (2015). Tunable Magnetization Dynamics in Interfacially Modified Ni81Fe19/Pt Bilayer Thin Film Microstructures. *Sci. Rep.*, 5, 17596.

[13] Marton, M., Zdravecká, E., Vojs, M., Ižák, T., Veselý, M., Redhammer, R., Varga, M., Šatka, A. (2009). Study of adhesion of carbon nitride thin films on medical alloy substrates. *Vacuum*, 84(1), 65–67.

[14] Zhang, G.P., Hübner, W., Lefkidis, G., Bai, Y., George, T.F. (2009). Paradigm of the time-resolved magneto-optical Kerr effect for femtosecond magnetism. *Nat. Phys.*, 5, 499–502.

[15] Silva, T.J., Lee, C.S., Crawford, T.M., Rogers, C.T. (1999). Inductive measurement of ultrafast magnetization dynamics in thin-film Permalloy. *J. Appl. Phys.*, 85, 7849.

[16] Vopson, M.M., Lees, K., Hall, M., Cain, M.G,, Stewart, M., Tran, Y. (2014). High frequency magnetization dynamics metrology using a pulsed field inductive microwave magnetometer. *Meas. Sci. Technol.*, 25(1), 15601–15607.